Textures in thin films of nematic liquid crystals induced by strongly focusing a circularly polarized laser

K. Miyakawa, A. Yoshinaga, and D. Ariyoshi
Department of Applied Physics, Fukuoka University, Fukuoka 814-0180, Japan
(Received 6 October 2010; revised manuscript received 17 January 2011; published 24 March 2011)

We investigate the rearrangement of the director in thin films of nematic liquid crystals caused by tightly focusing circularly polarized laser beams. We find either target or spiral patterns, depending on the topology of the director configuration at the position of the beam focus. The induced rearrangements of the director are governed by the viscosity of the media, the handedness of circular polarization, and the irradiation power of the laser. Experimental observations are interpreted using a model derived from nematic continuum theory.

DOI: 10.1103/PhysRevE.83.031704 PACS number(s): 61.30.Pq, 61.30.Gd, 42.70.Df

I. INTRODUCTION

When a laser beam propagates through a nematic liquid crystal (LC) with the local optical axis described by the molecular director, its electric field exerts a torque on the molecules. When the incident beam intensity exceeds a characteristic threshold, molecular reorientation occurs, known as the optical Fréedericksz transition (OFT) [1]. The phenomena of OFT have been extensively studied in various experimental geometries [2,3]. In particular, the polarization of the beam can be used as an effective parameter to control the reorientation of LCs. A linearly polarized laser beam can orient the director in the direction of laser polarization [4,5]. A circularly polarized laser beam normally incident on the homeotropic nematic LC film can cause a precession of the molecules around the beam propagation direction [6–8]. When a circularly polarized beam was incident on dye-doped nematic droplets, a nontrivial rotation was induced [9]. These phenomena are associated with the transfer of spin angular momentum from light to the medium.

Recently, optical tweezers with tightly focused laser beams have been applied to manipulation of molecular alignment in various LC systems—for example, manipulation of disclination lines and defects in LC films [10–12], spinning of micrometer-sized nematic LC droplets in water [13,14], and laser trapping of the colloidal particles of a refractive index that is lower compared to surroundings [15]. In a tightly focused laser beam, there are steep intensity gradients both perpendicular to the beam axis and along this axis, provided that the refractive index of the particle is larger than that of the surrounding medium. Thus laser tweezers have the advantage of exploring the new features of optically induced nonlinear effects in LC media.

In this paper, we address the possibility of the rearrangement of the director by tightly focusing a circularly polarized laser beam on the nematic LC films. Using crossed Nicols, we observe two distinct types of textures, target and spiral patterns, depending on the topology of the director configuration at the position of the beam focus. The formation of target and spiral patterns has also been reported in freely suspended smectic C films under shear flow [16–18] and an in-plane rotating electric field [19]. The handedness of the induced director arrangement is determined by the handedness of circular polarization. The laser-induced stationary patterns involved in OFT phenomena are reproduced using a model derived from the elastic free energy.

II. EXPERIMENT

The nematic liquid-crystal 4-n-pentyl-4-cyanobiphenyl (5CB) was dispersed in heavy water (D_2O) in a microtube. Here D_2O was used to avoid local heating produced by a tightly focused near-infrared laser beam. The mixture was stirred after adding the anionic surfactant (sodium linear alkyl benzensulfate, LAS) at a concentration of 43 mM above the critical micelle concentration of 1.2 mM to obtain radial molecular alignment. The nematic LC droplets containing LAS were then placed between two glass coverslips, resulting in the formation of depressed LC droplets, i.e., nematic disks of $30 \sim 150\ \mu$m in diameter and a few μm in thickness. When the microscopy image was taken through crossed Nicols at the position far from the glass boundaries, a distinctive four-armed texture was obtained as shown in Fig. 1(a). Molecules are aligned normal to the rim of the disk by the anchoring effect coming from the hydrophobicity of LAS. In a plane far from the cover-glass boundaries, therefore, molecules are radially aligned as schematically depicted in Fig. 1(b). Near the cover-glass boundaries, on the other hand, the director alignment in depressed droplets seems to be tilted-conical, where the fuzzy image of the four-armed texture was in fact observed. In the measurements all images of patterns have been taken at the position far from the cover-glass boundaries. Here we set x and y axes parallel (or perpendicular) to the directions of a crossed polarizer and analyzer.

A circularly polarized Nd:YVO4 laser (Spectra-Physics, BL106C) operating at $\lambda = 1064$ nm in a TEM_{00} mode was introduced into the inverted microscope (Nikon, TE300) and focused by the oil immersion objective lens ($100\times$, NA $= 1.3$). The microscope image was monitored by a charge coupled device (CCD) camera (chip size: 768×494 pixels) connected to the video recorder. We captured images at rates up to 1000FPS using a high-speed CCD camera (chip size: 640×480 pixels). Experiments were carried out at $24 \pm 0.5\ ^\circ$C.

III. RESULTS AND DISCUSSION

The molecular alignment in two-dimensional structures can be classified with topological index m [20]. In the radial alignment as shown in Fig. 1, we can distinguish two types regarding the topology of the in-plane director **n** by choosing the position of the beam focus. One is a defect-free arrangement that arises when the orientation of **n** is constant,

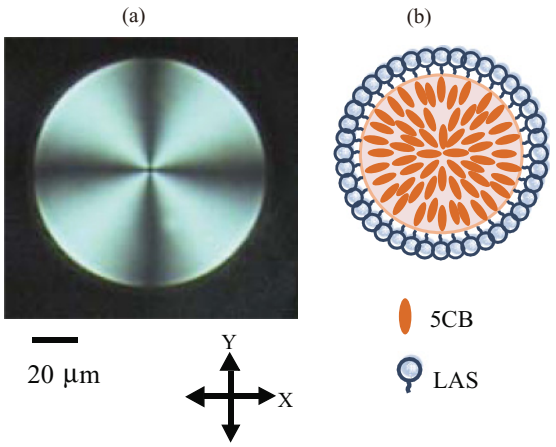

FIG. 1. (Color online) (a) Microscopy image of a radial 5CB disk of 103 μm taken under crossed polarizers. (b) Schematic presentation of radial molecular alignment. The double-headed arrow represents the direction of the polarizer and analyzer.

so that $m = 0$ holds. This configuration is realized in the region far from the core of the defect, where **n** can be approximately regarded as constant around the very narrow region such as the focused region. The other is the arrangement around the core of a defect of $m = +1$, where **n** has a radial symmetry.

When the beam was focused on the region of $m = 0$ far from the core of the defect, rings sequentially gushed out from the beam spot and grew into a stationary time-independent target pattern. Figure 2 shows stationary patterns depending on the irradiation power of laser. The number of rings increases with an increase in irradiation power. Such a concentric ring profile is independent of the handedness of circular polarization of the incident beam. When the laser irradiation was turned off, ring textures shrunk toward its center.

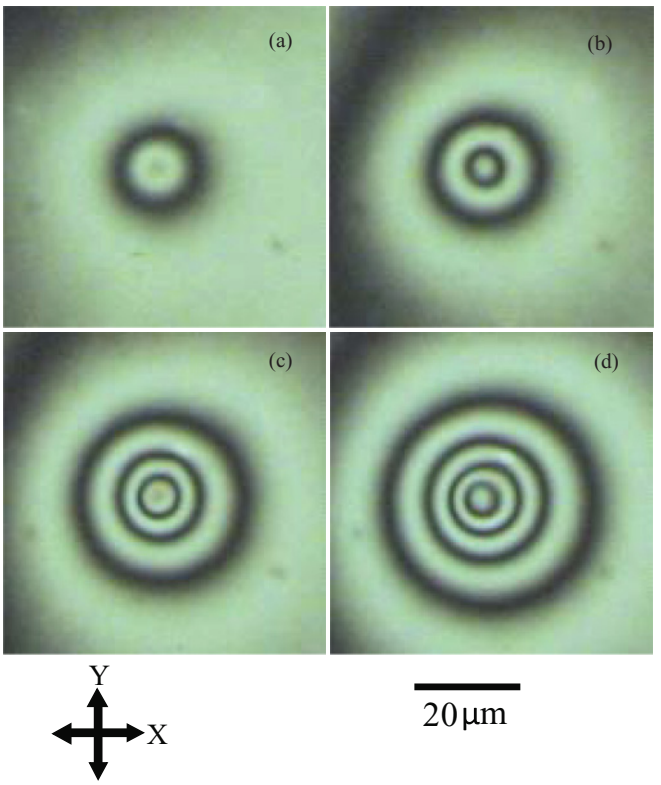

FIG. 2. (Color online) Concentric ring textures as functions of the irradiation power of right-circularly polarized laser taken under crossed polarizers; (a) 75 mW, (b) 170 mW, (c) 200 mW, and (d) 300 mW. Every pattern was taken approximately 60 s after the beginning of irradiation.

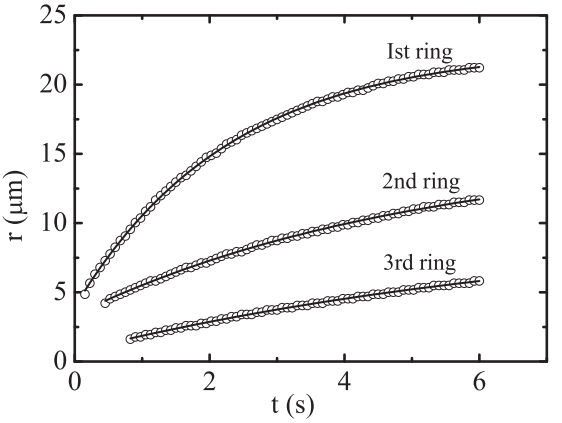

FIG. 3. Ring radii as functions of time at the laser power of 340 mW. The radii of the first, second, and third rings grow exponentially with time constants of 2.3 s, 5.1 s, and 7.8 s, respectively.

Figure 3 shows the time courses of the ring radii of the target pattern. The time course of the radius of the most outer ring (MOR) can be fitted with a simple exponential curve with the time constant of 2.3 s. Other rings in the target pattern also showed an exponential growth with larger time constants.

We investigated the change in properties of the system by adding an increasing quantity of D_2O to the liquid crystal. Figure 4 shows the radius of the MOR r vs the volume fraction of D_2O ϕ_w at the fixed irradiation power of 340 mW. No rings are observed in the LC medium without D_2O. This seems to be attributable to the glass anchoring which would impose a strong planar alignment. With an increase in quantity of D_2O without the surfactant (LAS), the ring is formed, but its radius does not become so large and tends to saturate. This

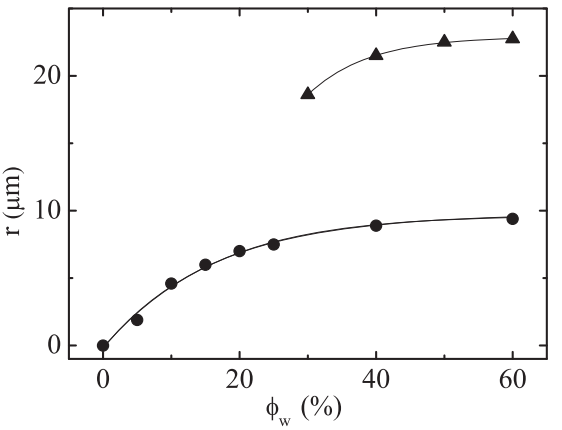

FIG. 4. Radius of the most outer ring of the target pattern as a function of volume fraction of D_2O in the LC samples without the surfactant (circles) and with the surfactant (triangles) at an irradiation power of 340 mW. The lines are guides for the eye.

implies that the glass anchoring is weakened to some extent by adding D_2O, but the molecules of LC are still interacting with the glass surface even at a large ϕ_w. This may be due to that a homogenous thin water film is not formed at the glass surface, since water and the LC are immiscible. When D_2O contains a fixed concentration of LAS, in contrast, the radius is increased by a factor slightly larger than two, compared with the samples without LAS. At large ϕ_w, the radius becomes almost independent of ϕ_w. This seems to indicate that the addition of LAS in D_2O causes the dewetting of LC from the interface between a water-immiscible LC and the glass surface and changes the tilt of the tilted-conical anchoring at the water boundary, presumably resulting in the reduction of the effective 2D elastic constant acting for transverse deformations. Then the director can be free to reorient by application of a strongly focused laser.

When the target pattern evolved from the beginning of laser irradiation and consequently the MOR approached one of the four-armed brushes as shown in Fig. 1(a), the MOR repelled or drew that brush, depending on the handedness of the circular polarization of the beam. Figure 5 shows the case in which the circularly polarized beam was focused on the first quadrant defined by a single four-armed texture. In the case of right-handed polarization, the MOR necessarily draws the brush pointing along the x axis [Fig. 5(b)] and is consequently assimilated into that brush [Fig. 5(c)], indicating that the director on the MOR orients in the x direction. When the handedness of polarization was switched from right to left,

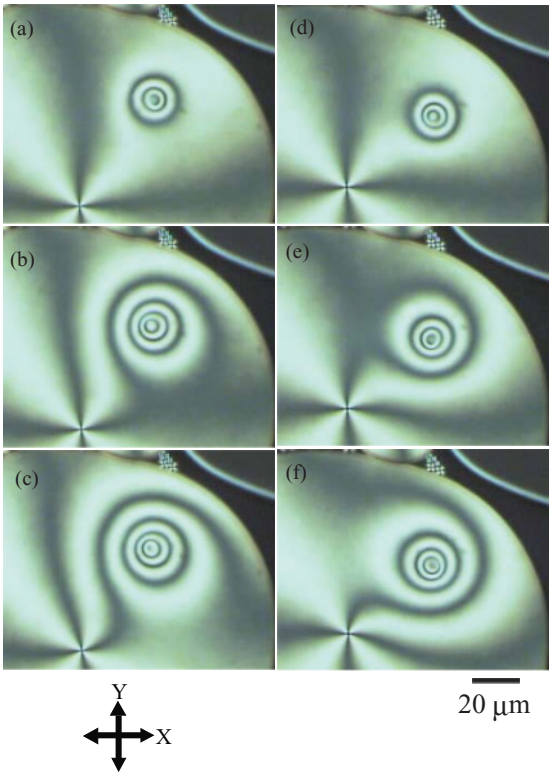

FIG. 5. (Color online) Sequential images of time evolution of multiple-ring textures taken under crossed polarizers. Here (a)–(c) and (d)–(f) are due to right- and left-circularly polarized lasers, respectively.

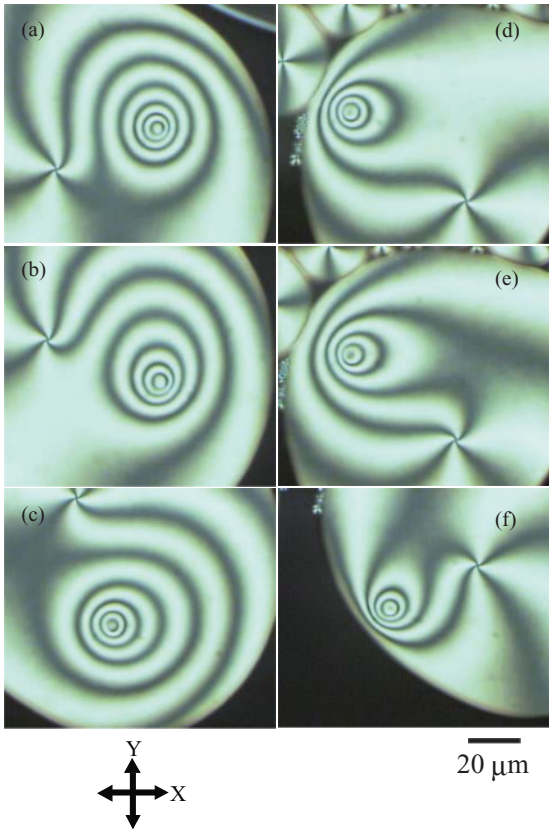

FIG. 6. (Color online) Sequential images of textures generated by shifting the focus position of right-circularly polarized beam around the defect core, (a)–(c) clockwise and (d)–(f) counterclockwise.

in contrast, the MOR necessarily drew the brush pointing along the y axis, as shown in Figs. 5(d)–5(f). This indicates that the director on the MOR orients in the y direction.

Furthermore, starting with the state shown in Fig. 5(c), we moved the focus position of the right-circularly polarized beam around the defect core. A clockwise shift caused the MOR to draw the brush pointing in the $-y$ direction [Fig. 6(a)], to be assimilated into that brush [Fig. 6(b)], and then to draw freshly the brush pointing in the $-x$ direction [Fig. 6(c)]. These results indicate that the director in the MOR in Figs. 6(a) and 6(b) orients in the $-y$ and $-x$ directions, respectively. On the other hand, a counterclockwise shift of the beam spot caused the MOR to repel the brush pointing in the x direction [Fig. 6(d)]. The plucked brush was broken and spontaneously closed [Fig. 6(e)], resulting in the formation of the fresh MOR on which the director points in the x direction [Fig. 6(f)]. In contrast, a clockwise or counterclockwise shift of the left-circularly polarized beam spot caused opposite behaviors. From these observations, we conclude that the orientation of $\mathbf{n}$ changes by $\pi/2$ between adjacent rings, and that the orientation of $\mathbf{n}$ on each ring differs by $\pi/2$ from that on the corresponding ring induced by the beam with the opposite circularity.

When the beam was focused on the core of an $m = +1$ defect, a stationary time-independent spiral texture with four dark brushes was generated, as shown in Fig. 7. On the rim of the LC disk the molecules are fixed normal to the rim, and

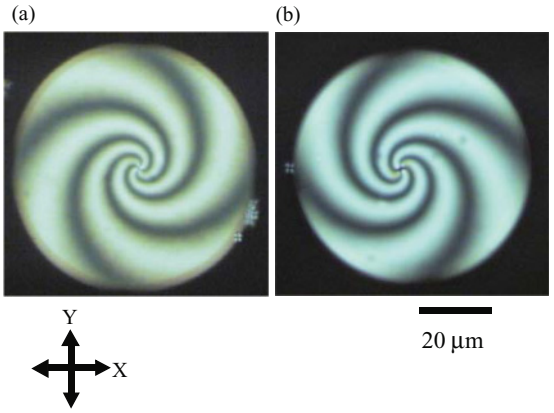

FIG. 7. (Color online) Spiral textures with four dark brushes generated by (a) left- and (b) right-circularly polarized beams focused on the core of an $m = +1$ defect, where the irradiation power of the laser is 340 mW.

around the beam spot they are forced to rotate by a certain angle. The degree of twist depends on the irradiation power of the incident beam. The sense of the spiral is determined by the handedness of circular polarization. This implies the occurrence of a spin angular momentum transfer from the laser beam to the LC. However, in a rotationally invariant geometry such as the radial symmetry there is no angular momentum coupling between light and matter [21]. Therefore, some origin that causes such an angular momentum coupling should be present. Twisted deformation was remarkable when the focused point of the beam was located far from two cover-glass boundaries, where the director approximately takes a planar orientation. Near the glass boundaries, in contrast, such a deformation became weakened. In this region the alignment of the director is perhaps tilted-conical. As the trapping laser beam has a finite extension and depth of focus, there is probably some residual imperfection around the beam axis. Such a breaking of the cylindrical symmetry seems to contribute to the occurrence of angular momentum coupling between light and the LC. Spiral patterns have also been observed in homeotropic LC thin films subject to focused circularly polarized light [22].

Generation of target and spiral patterns is deeply related with distortions of the in-plane director arrangement caused in the focused region. In LC media in which the dielectric constants parallel $\epsilon_\parallel$ and perpendicular $\epsilon_\perp$ to the local director are different, the director favors alignment parallel or perpendicular to an external electric field. according to whether the anisotropy $\epsilon_a = \epsilon_\parallel - \epsilon_\perp$ is positive or negative, respectively [20]. Since ϵ_a in the nematic phase of 5CB is positive, the director prefers alignment parallel to the direction of laser polarization in the optical field. When the laser beam is circularly polarized, the electric field of light $\mathbf{E}$ rotates at high frequency. The characteristic time for the rotation of the director is quite long compared to the periodicity of the field, so that the director cannot follow the too rapid rotation of the field. The director is then subject to the optical torque proportional to $\langle(\mathbf{n}\cdot\mathbf{E})(\mathbf{n}\times\mathbf{E})\rangle_t$ on an average, where the brackets indicate time averaging. This will cause the director to rotate up to a certain angle which is determined by a balance among the optical torque, the Frank elastic torque, and the viscous torque acting on the director. After a relaxation time from the beginning of laser irradiation, the arrangement of molecules in the bulk reaches a stationary state on the whole, and time-independent patterns consequently appear. The stronger the irradiation power of the laser, the larger the distortion angle of the director on the beam spot becomes, resulting in an increase of the number of rings for the $m = 0$ target and of the extent of twist for the $m = +1$ spiral.

To describe the phenomena observed, we calculate the distortion free energy of the in-plane director [20], which is isomorphic to that of two-dimensional smectic C [16]. We use cylindrical coordinates (r, ϕ, z) and introduce the angle ψ between the local optical axis and the radial direction $\mathbf{r}$. Then the in-plane director $\mathbf{n}$ is given by $n_r = \cos\psi$ and $n_\phi = \sin\psi$. The relation between ϕ and ψ is then given by

$$\psi = (m-1)\phi + f(r), \tag{1}$$

where $f(r)$ is a function of r only. Assuming the one-constant approximation for elastic constants, we obtain the elastic free energy (per unit length along z)

$$F_{\rm el} = \frac{K}{2}\int\left[\left(1+\frac{\partial\psi}{\partial\phi}\right)^2 + \left(r\frac{\partial\psi}{\partial r}\right)^2\right]\frac{dr}{r}d\phi, \tag{2}$$

where K is the elastic constant. We assume that the rotation angle of the director on the beam spot is ψ_0 and the equilibrium orientation angle of the director in the bulk is ψ_c. The boundary condition for the configuration of $m = 0$ is then given by $\psi = -\phi + \psi_0$ on the beam spot of the radius r_0 of around 0.5 μm and $\psi = -\phi + \psi_c$ at a cutoff length r_c at which the director recovers the equilibrium orientation ψ_c in the bulk, where r_c is several decades of μm. On the other hand, the boundary condition for the $m = +1$ case is given by $\psi = \psi_0$ at r_0 and $\psi = 0$ at r_c. Minimizing Eq. (2) with these boundary conditions leads to the static solutions

$$\psi = -\phi + (\psi_0 - \psi_c)\frac{\ln(r/r_c)}{\ln(r_0/r_c)} + \psi_c \quad \text{for } m = 0 \tag{3}$$

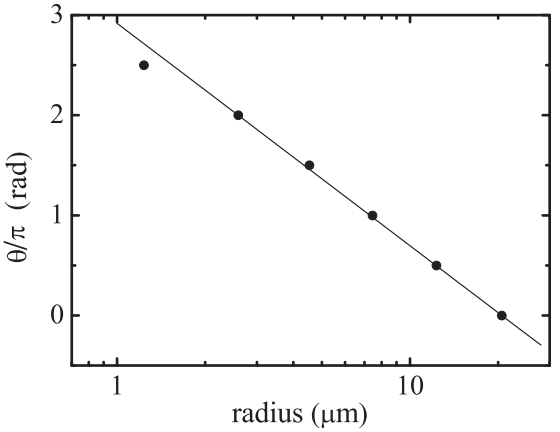

FIG. 8. Azimuthal angle of the director as a function of the ring radius. The solid line represents the fit of data to Eq. (3) yielding the relative distortion angle $\Delta\psi = \psi_0 - \psi_c \simeq 3.8\pi$ with $r_0/r_c \sim 1.88\times10^{-2}$.

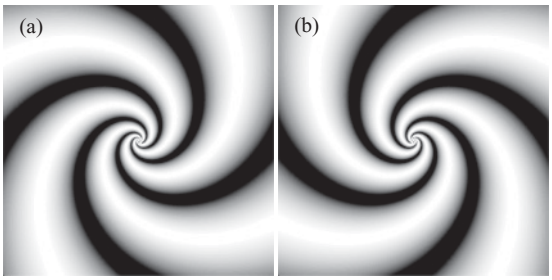

FIG. 9. Intensity profiles of spiral patterns depending on the sign of the distortion angle ψ_0 when $r_c = 30$ μm and $r_0 = 0.5$ μm: (a) $\psi_0 = 2.0\pi$; (b) $\psi_0 = -2.0\pi$.

and

$$\psi = \psi_0 \frac{\ln(r/r_c)}{\ln(r_0/r_c)} \quad \text{for } m = +1. \tag{4}$$

For the $m = 0$ target, the azimuthal angle of the director θ, given by $\theta = \psi + \phi$, does not depend on the radial direction but only the distance from the beam spot. Equation (3) predicts a linear relation between θ and $\ln r$. In Fig. 8, θ is plotted against the logarithmic ring radii of a sextuple ring pattern. Here, for simplicity, the value of θ on the MOR is taken as zero, since it must be zero or $\pi/2$. The linear behavior predicted by Eq. (3) is well observed and allows determination of the parameters, such as the relative distortion angle $\Delta\psi = \psi_0 - \psi_c$ and the ratio r_0/r_c.

For the $m = +1$ spiral, θ depends on both the radial direction and the distance from the beam spot. Figure 9 shows two spirals differing in sign of the rotation angle ψ_0. The extent of twist depends on the magnitude of ψ_0. One can see that the handedness of the spiral pattern is determined by the sign of ψ_0. This is similar to the experimental observations that the handedness of the spiral pattern is governed by that of circular polarization.

In contrast the intensity profile of the target pattern does not depend on the sign of $\Delta\psi$ but only the magnitude of $\Delta\psi$. The arrangement of the director exhibits a winding depending on the sign of $\Delta\psi$, although pattern profiles are identical, as shown in Fig. 10. The orientation of the director θ changes by $\pi/2$ between succeeding rings, and differs by $\pi/2$ from that on the corresponding ring of patterns with $\Delta\psi$ of the opposite sign.Thus Eqs. (3) and (4) nicely reproduce the experiment ally observed patterns, indicating that a limited rotation of the director induced on the beam spot is responsible for generation of textures.

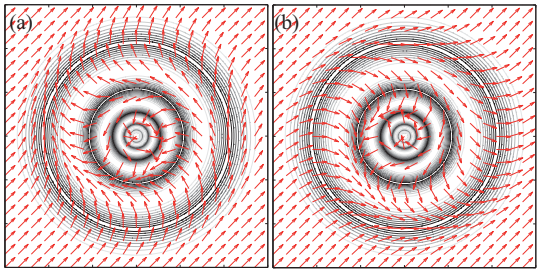

FIG. 10. (Color online) Contour plots of intensity through the crossed polarizers and director field lines of target patterns depending on the sign of the relative distortion angle $\Delta\psi = \psi_0 - \psi_c$ when $r_c = 30$ μm and $r_0 = 0.5$ μm: (a) $\Delta\psi = 3.0\pi$; (b) $\Delta\psi = -3.0\pi$.

IV. CONCLUSION

We have investigated the rearrangement of the director in the nematic LC droplets caused by the focused laser beam. We have found two distinct types of stationary patterns depending on the topological index m. One is a target pattern in the $m = 0$ geometry and another is a spiral pattern around a central defect with $m = +1$. These are similar to shear-flow-induced patterns in freely suspended smectic C liquid crystal films [16]. We have demonstrated experimentally for the first time that observed phenomena are entirely attributable to limited rotations of the director involved in the optical Fréedericksz transition, using a model that provides a reasonable description of the observations. Such a generation of microscopic textures due to a coupling between the director field and the optical field is permitted only by using the optical tweezer. Other abilities of optical tweezers, such as optical trapping and manipulation, will further open new possibilities for studies of nonlinear dynamics of disclinations and defects in LC films.

ACKNOWLEDGMENTS

This work was supported in part by a Grant-in-Aid for Scientific Research from the Ministry of Education, Culture, Sports, Science, and Technology of Japan (Grant No. 21540403), and was also supported in part by the Central Research Institute of Fukuoka University.

[1] A. S. Zolot'ko, V. F. Kitaeva, N. Kroo, N. I. Sobolev, and L. Csillag, Sov. Phys. JETP Lett. **32**, 158 (1980).
[2] I. C. Khoo and S. T. Wu, *Optics and Nonlinear Optics of Liquid Crystals* (World Scientific, Singapore, 1993), Vol. 1.
[3] F. Simoni and O. Francescangeli, J. Phys. Condens. Matter **11**, R439 (1999).
[4] S. D. Durbin, S. M. Arakelian, and Y. R. Shen, Phys. Rev. Lett. **47**, 1411 (1981).
[5] W. M. Gibbons, P. J. Shannon, Shao-Tang Sun, and B. J. Swetlin, Nature (London) **351**, 49 (1991).
[6] E. Santamato, B. Daino, M. Romagnoli, M. Settembre, and Y. R. Shen, Phys. Rev. Lett. **57**, 2423 (1986).
[7] E. Santamato, G. Abbate, P. Maddalena, L. Marrucci, and Y. R. Shen, Phys. Rev. Lett. **64**, 1377 (1990).
[8] L. Marrucci, G. Abbate, S. Ferraiuolo, P. Maddalena, and E. Santamato, Phys. Rev. A **46**, 4859 (1992).
[9] C. Manzo, D. Paparo, L. Marrucci, and I. Jánossy, Phys. Rev. E **73**, 051707 (2006).
[10] J. Hotta, K. Sasaki, and H. Masuhara, Appl. Phys. Lett. **71**, 2085 (1997).

[11] M. Kojima, J. Yamamoto, K. Sadakane, and K. Yoshikawa, Chem. Phys. Lett. **457**, 130 (2008).

[12] I. I. Smalyukh, B. I. Senyuk, S. V. Shiyanovskii, O. D. Lavrentovich, A. N. Kuzmin, A. V. Kachynski, and P. N. Prasad, Mol. Cryst. Liq. Cryst. **450**, 79 (2006).

[13] S. Juodkazis, M. Shikata, T. Takahashi, S. Matsuo, and H. Misawa, Appl. Phys. Lett. **74**, 3627 (1999); Jpn. J. Appl. Phys. **38**, L518 (1999).

[14] E. Brasselet, N. Murazawa, S. Juodkazis, and H. Misawa, Phys. Rev. E **77**, 041704 (2008).

[15] I. Muševič, M. Škarabot, D. Babič, N. Osterman, I. Poberaj, V. Nazarenko, and A. Nych, Phys. Rev. Lett. **93**, 187801 (2004).

[16] P. E. Cladis, Y. Couder, and H. R. Brand, Phys. Rev. Lett. **55**, 2945 (1985).

[17] P. E. Cladis, P. L. Finn, and H. R. Brand, Phys. Rev. Lett. **75**, 1518 (1995).

[18] R. Stannarius, C. Bohley, and A. Eremin, Phys. Rev. Lett. **97**, 097802 (2006).

[19] D. R. Link, L. Radzihovsky, G. Natale, J. E. Maclennan, N. A. Clark, M. Walsh, S. S. Keast, and M. E. Neubert, Phys. Rev. Lett. **84**, 5772 (2000).

[20] P. G. de Gennes and J. Prost, *The Physics of Liquid Crystals* (Clarendon Press, Oxford, 1993).

[21] L. Marrucci, C. Manzo, and D. Paparo, Phys. Rev. Lett. **96**, 163905 (2006).

[22] E. Brasselet, Opt. Lett. **34**, 3229 (2009).